

Dynamics of an axisymmetric body spinning on a horizontal surface. III. Geometry of steady state structures for convex bodies

M Branicki, H.K Moffatt and Y Shimomura

Proc. R. Soc. A 2006 **462**, doi: 10.1098/rspa.2005.1586, published 8 February 2006

References

This article cites 8 articles, 2 of which can be accessed free
<http://rspa.royalsocietypublishing.org/content/462/2066/371.full.html#ref-list-1>

Article cited in:
<http://rspa.royalsocietypublishing.org/content/462/2066/371.full.html#related-urls>

Email alerting service

Receive free email alerts when new articles cite this article - sign up in the box at the top right-hand corner of the article or click [here](#)

Dynamics of an axisymmetric body spinning on a horizontal surface. III. Geometry of steady state structures for convex bodies

BY M. BRANICKI^{1,*}, H. K. MOFFATT¹ AND Y. SHIMOMURA²

¹*Department of Applied Mathematics and Theoretical Physics,*

Wilberforce Road, Cambridge CB3 0WA, UK

²*Department of Physics, Keio University, Hiyoshi Yokohama 223-8521, Japan*

Following parts I and II of this series, the geometry of steady states for a general convex axisymmetric rigid body spinning on a horizontal table is analysed. A general relationship between the pedal curve of the cross-section of the body and the height of its centre-of-mass above the table is obtained which allows for a straightforward determination of static equilibria. It is shown, in particular, that there exist convex axisymmetric bodies having arbitrarily many static equilibria. Four basic categories of non-isolated fixed-point branches (i.e. steady states) are identified in the general case. Depending on the geometry of the spinning body and its dynamical properties (i.e. position of centre-of-mass and inertia tensor), these elementary branches are differently interconnected in the six-dimensional system phase space and form a complex global structure. The geometry of such structures is analysed and topologically distinct classes of configurations are identified. Detailed analysis is presented for a spheroid with displaced centre-of-mass and for the tippe-top. In particular, it is shown that the fixed-point structure of the flip-symmetric spheroid, discussed in part I, represents a degenerate configuration whose degeneracy is destroyed by breaking the symmetry. For the spheroid, there are in general nine distinct classes of fixed-point structures and for the tippe-top there are three such structures. Bifurcations between these classes are identified in the parameter space of the system.

Keywords: rigid body dynamics; dynamical systems; non-isolated fixed-points; spinning bodies

1. Introduction

In parts I and II of this series (Moffatt *et al.* 2004; Shimomura *et al.* 2005), various aspects of dynamics of an axisymmetric body spinning on a horizontal table were analysed. In part I, the governing six-dimensional dynamical system was derived and stability analysis of steady states for a ‘flip-symmetric’ spheroid (whose density distribution is mirror-symmetric with respect to the

* Author for correspondence (mb388@damtp.cam.ac.uk).

plane through the centre normal to the axis of symmetry) were presented. It was also shown, following Moffatt & Shimomura (2002), that under the so-called ‘gyroscopic balance’ condition which holds in the high-spin situation, the Jellett constant was ‘adiabatically’ conserved for such spheroids. This adiabatic invariance enabled dramatic reduction of the six-dimensional system, leading to a first-order differential equation which described the rise of the centre-of-mass of the spinning spheroid. This paradoxical ‘rising phenomenon’ was associated with the presence of weak friction (measured by a dimensionless parameter $\mu \ll 1$) at the point of contact and occurred on a slow time-scale $O(\mu^{-1})$. Part II focused on the possibility of a self-induced jumping whereby, for sufficiently large initial precession and for appropriate values of the system parameters, amplification of certain oscillatory modes resulted in the spheroid losing contact with the table during the slow rising motion. These rapid oscillations, occurring on an $O(1)$ time-scale and identified earlier in the stability analysis of part I, were further analysed by the WKB method in order to obtain the time-dependence of the normal reaction acting on the spinning body and determine the circumstances leading to this jumping phenomenon.

In the present paper, we extend the analysis to a consideration of general convex axisymmetric bodies of axisymmetric density distribution, and the structure of the corresponding steady states is studied. First, we establish a relationship between the pedal curve of the cross-section of the body and the height of its centre-of-mass above the table. This allows for a straightforward determination of static equilibria directly from the pedal curve and we illustrate this for a few model contours; an example of a convex axisymmetric body with an arbitrary number of static equilibria is also presented. We later identify basic categories of ‘dynamic’ equilibria (i.e. steady states), which correspond to branches of non-isolated fixed-points, in the general axisymmetric case. These branches are usually interconnected and form a complex global structure in the system phase space. It turns out that, depending on the geometry of the spinning body, the position of its centre-of-mass and its principal moments of inertia, many topologically distinct configurations of the fixed-point branches are possible. Even for the prototype problem of a spheroid with displaced centre-of-mass, discussed in detail in §4, there are nine topologically distinct configurations. These all bifurcate into each other as the system parameters are varied and we derive a bifurcation diagram describing these transitions in the parameter space. In particular, we show that the fixed-point structure for the flip-symmetric spheroid represents a degenerate (structurally unstable) configuration which is destroyed when the symmetry is broken. The tippe-top is another well known example of a spinning body that, if constructed properly, exhibits the ‘rising phenomenon’ similar to that observed for the spinning spheroid. We discuss this important case separately and show that for such a geometry, there are only three distinct classes of fixed-point configurations.

It will be shown in the subsequent publication (part IV) that there is an intricate relationship between the geometry of the fixed-point structures and the stability properties of individual branches which predetermines the dynamical behaviour of the spinning body.

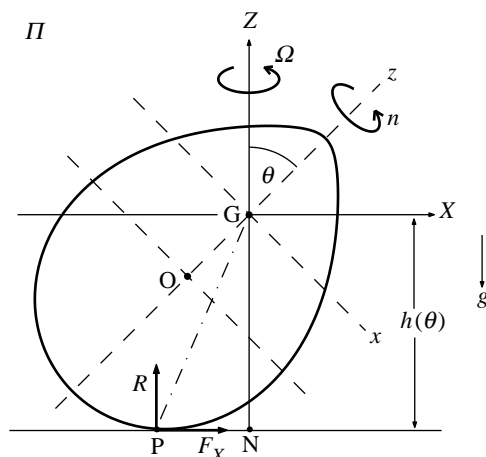


Figure 1. An axisymmetric body with centre-of-mass G and centre-of-volume O spins on a horizontal table with a point of contact P and pedal point N (see §3*a*). Location of G is determined by the (axisymmetric) density distribution. The axis of symmetry $Gz = (Oz)$ and the axis GZ define a plane Π (containing GP) which precesses about GZ with angular velocity Ω . $GXYZ$ is a rotating frame of reference, with GX horizontal in the plane Π . The height of G above the table is $h(\theta)$ and the coordinates of P are $X_P = dh/d\theta$, $Y_P = 0$, $Z_P = -h(\theta)$. The forces acting on the body are its weight $-Mg\mathbf{K}$, the normal reaction \mathbf{R} at P , and the (horizontal) frictional force \mathbf{F} at P .

2. Geometry and kinematics of the problem

Let us first repeat the essential notations and equations for the problem, as presented in part I. We consider the dynamics of a rigid axisymmetric body with cross-section S , centre-of-volume O and centre-of-mass G which moves on a horizontal table, making sliding and/or rolling contact at the point P (figure 1).

Let $h(\theta)$ be the height of G above the table; this function is determined by the cross-section S and by the (axisymmetric) density distribution within S . In the following, we assume that S is strictly convex and that h , $dh(\theta)/d\theta$, $d^2h(\theta)/d\theta^2$ are continuous; in particular, we require $dh(\theta)/d\theta|_{\theta=0,\pi} = 0$.

Six variables, $\Xi = (U, V, \Omega, A, \theta, n)$, are needed to define the state of motion of the body: (U, V) are the X - and Y -components of velocity of G , Ω is the rate of precession of Gz about GZ , θ is the angle between Gz and GZ , $A = \dot{\theta}$, and n is the spin (i.e. the component of angular velocity about Gz). We use dimensionless variables based on $(M, b, (b/g)^{1/2})$ as units of mass, length and time, where M is the mass of the body, b is its radius of cross-section in the plane Gxy , and g is the acceleration of gravity.

With Gx in the plane defined by Gz and the vertical GZ , we may use $Gxyz$ as a rotating frame of reference. Alternatively, we may use $GXYZ$, where GX is horizontal and GY coincides with Gy . As derived in Moffatt & Shimomura (2002), the coordinates of P in $GXYZ$ are given by

$$\mathbf{X}_P = (X_P, Y_P, Z_P) = (h_\theta, 0, -h), \quad (2.1)$$

where $h_\theta = dh/d\theta$, or equivalently, in the body frame of reference $Gxyz$, by:

$$\mathbf{X}_P = (x_P, y_P, z_P) = (h \sin \theta + h_\theta \cos \theta, 0, -h \cos \theta + h_\theta \sin \theta). \quad (2.2)$$

Note that for a general axisymmetric body $x_P=0$ only at $\theta=0, \pi$. The velocity of the point P (of the body) is

$$\mathbf{U}_P = U_P \mathbf{I} + V_P \mathbf{j} + W_P \mathbf{K}, \quad (2.3)$$

where $\mathbf{I}, \mathbf{J}(=\mathbf{j}), \mathbf{K}$ are unit vectors in the directions GX, GY(=Gy) and GZ and

$$U_P = U - h\Lambda, \quad (2.4a)$$

$$V_P = V + (n - \Omega \cos \theta)(h \sin \theta + h_\theta \cos \theta) + \Omega h_\theta, \quad (2.4b)$$

$$W_P = W - \Lambda h_\theta. \quad (2.4c)$$

W is the vertical component of velocity of G. The horizontal velocity components, U_P and V_P , are in general non-zero since we allow for slip. However, for so long as the body remains in contact with the table, we have $W_P=0$ which implies

$$W = \Lambda h_\theta. \quad (2.5)$$

The normal reaction R is then given by

$$R = 1 + \dot{W} = 1 + \frac{d(\Lambda h_\theta)}{dt}. \quad (2.6)$$

Following part I, the governing evolution equations can be cast in the form of a sixth-order nonlinear dynamical system which we arrange in the standard form $\dot{\Xi} = \mathcal{F}(\Xi)$

$$\dot{U} = \Omega V + F_X, \quad (2.7a)$$

$$\dot{V} = -\Omega U + F_y, \quad (2.7b)$$

$$\dot{\Omega} = [-2A\Omega\Lambda \cos \theta + Cn\Lambda + F_y z_P](A \sin \theta)^{-1}, \quad (2.7c)$$

$$\dot{\Lambda} = [\Omega \sin \theta(A\Omega \cos \theta - Cn) - Rh_\theta - hF_X]A^{-1}, \quad (2.7d)$$

$$\dot{\theta} = \Lambda, \quad (2.7e)$$

$$\dot{n} = C^{-1} x_P F_y, \quad (2.7f)$$

where F_X and $F_y(=F_Y)$ are the components of the frictional force $\mathbf{F}=F_X \mathbf{I}+F_y \mathbf{j}$ at P and (A, A, C) are the (dimensionless) principal moment of inertia of the spinning body at G. In this formulation, the dynamical evolution of the spinning body from the initial state Ξ_0 is represented by an appropriate trajectory $\Xi(t)$ in the six-dimensional phase space of the system (2.7a-f) which has, in general, two important symmetries:

$$\mathcal{F}(U, V, \Omega, \Lambda, \theta, n) = \mathcal{F}(U, -V, -\Omega, \Lambda, \theta, -n) = \mathcal{F}(-U, -V, \Omega, -\Lambda, -\theta, n). \quad (2.8)$$

In order to complete the specification of the problem, we neglect rolling friction and assume that $\mathbf{F} = -\mu R \mathbf{f}(\mathbf{U}_P)$, where \mathbf{f} is an odd function of \mathbf{U}_P . The reaction R may be then expressed, via (2.7a-c), as a function of the system variables as

$$R = R(U, \Omega, \Lambda, \theta, n) = \frac{1 + h_{\theta\theta}\Lambda^2 + \Omega h_\theta \sin \theta(A\Omega \cos \theta - Cn)A^{-1}}{1 + h_\theta(h_\theta - \mu h f_X(\mathbf{U}_P))A^{-1}}, \quad (2.9)$$

where $h_\theta = dh/d\theta$, $h_{\theta\theta} = d^2h/d\theta^2$.

As discussed in part II, there are circumstances when a trajectory crosses the surface $R=0$ and the body enters a different dynamical regime of ‘free’ rotation

under the action of gravity (with $R \equiv 0$). We restrict the following analysis to the situation when $R \geq 0$ so that the body remains in contact with the table throughout the evolution. As was shown in part II, this scenario generally¹ corresponds to the situation when the initial kinetic energy of the spinning body does not exceed a certain threshold value.

3. Steady states

The steady states of the system (2.7a–c) are the fixed-points, where

$$\dot{\mathcal{E}} = \mathcal{F}(\mathcal{E}) = 0. \quad (3.1)$$

These steady states are either ‘static equilibria’, when the kinetic energy of the body is identically zero and the potential energy is extremal, or ‘dynamic equilibria’ when the kinetic and the potential energy of the spinning body are both constant (and non-zero). We do not consider here more general time-dependent equilibria (for example, limit-cycles, invariant tori, etc.) for which the total mechanical energy (kinetic plus potential) is constant.

In this section, we first establish a geometrical relationship between the so-called pedal curve and the height function h , which provides an easy way of determining all the static equilibria for an arbitrary cross-section S . We later classify all the steady states that exist for a general convex axisymmetric body. In particular, it is shown that the distinct classes of steady states, generally, form a connected structure in the phase space where the static equilibria serve as connection points between different branches of non-isolated dynamic equilibria.

(a) Relationship between the pedal curve, the height function and static equilibria

Let $S = (\mathcal{X}(l), \mathcal{Z}(l))$, $l \in [0, 2\pi]$ be the cross-section of the axisymmetric body in the frame of reference $Oxyz$ fixed at the centre-of-volume O (see figure 1). We assume here that \mathcal{X} and \mathcal{Z} are smooth periodic functions of l and that the contour S is strictly convex, i.e.

$$\mathcal{Z}'\mathcal{X}'' - \mathcal{X}'\mathcal{Z}'' \neq 0, \quad (3.2)$$

where $\mathcal{X}' = d\mathcal{X}/dl$, $\mathcal{Z}' = d\mathcal{Z}/dl$, $\mathcal{X}'' = d^2\mathcal{X}/dl^2$, $\mathcal{Z}'' = d^2\mathcal{Z}/dl^2$.

Consider now the pedal curve (Salmon 1873) $N = (x_N, z_N)$ of S relative to the pedal point $G = (0, \hat{\rho})$ (i.e. centre-of-mass in $Oxyz$). This is the locus of the intersection of the perpendicular from G to a tangent to S , and can be written in parametric form as

$$x_N = \frac{(\hat{\rho} - \mathcal{Z})\mathcal{X}'\mathcal{Z}' + \mathcal{X}\mathcal{Z}'^2}{\mathcal{X}'^2 + \mathcal{Z}'^2}, \quad z_N = \frac{\hat{\rho}\mathcal{Z}'^2 - \mathcal{X}\mathcal{X}'\mathcal{Z}' + \mathcal{Z}\mathcal{X}'^2}{\mathcal{X}'^2 + \mathcal{Z}'^2}. \quad (3.3)$$

It is then evident that, since G lies inside the convex contour S , the pedal curve N lies outside S and is tangent to it at points, where

$$Q \equiv \mathcal{X}\mathcal{X}' + (\mathcal{Z} - \hat{\rho})\mathcal{Z}' = 0. \quad (3.4)$$

¹We exclude here the possibility of choosing initial conditions that would lead to immediate jumping (i.e. $R(U_0, \Omega_0, A_0, \theta_0, n_0) \leq 0$) as opposed to the jumping caused by self-induced oscillations.

Note also that the distance from G to N is given by the height function h which, using (3.3), can be written as

$$h(l) = \sqrt{x_N^2 + (z_N - \hat{\rho})^2} = \frac{|\mathcal{X}\mathcal{Z}' - (\mathcal{Z} - \hat{\rho})\mathcal{X}'|}{\sqrt{\mathcal{X}'^2 + \mathcal{Z}'^2}}, \quad (3.5)$$

where $l(\theta)$ is given implicitly by the solution of

$$\tan \theta = -\frac{x_N(l)}{z_N(l) - \hat{\rho}} = \frac{\mathcal{Z}'}{\mathcal{X}'}. \quad (3.6)$$

Note that (3.6) implies that $dl/d\theta \neq 0$, if (3.2) is satisfied.

The points where $h_\theta = 0$ determine static equilibria of the body S . Moreover, it can be easily checked, using (3.5) and (3.6) that these points correspond to the solutions $Q(l) = 0$, where the pedal curve is tangent to the contour S .²

Consider first, by way of example, the important case of a spheroid with axisymmetric mass distribution. In this case, the cross-section can be written in the parametric form

$$S = (\sin l, a \cos l), \quad l \in [0, 2\pi], \quad (3.7)$$

where a is the ratio of the principal axes of the spheroid. The pedal curve (3.3) with respect to $G = (0, \hat{\rho})$ is then given by

$$x_N = \frac{a \sin l (a - \hat{\rho} \cos l)}{a^2 \sin^2 l + \cos^2 l}, \quad z_N = \frac{a(\cos l + a \hat{\rho} \sin^2 l)}{a^2 \sin^2 l + \cos^2 l}. \quad (3.8)$$

Note that there are always two ‘vertical’ static equilibria with P located on the axis of symmetry (i.e. $l=0$ and π) regardless of the location of the pedal point G. From (3.7) and (3.4), we find that there are also two ‘intermediate’ static equilibria located symmetrically at

$$l = \pm \cos^{-1} \left(\frac{a\hat{\rho}}{a^2 - 1} \right), \quad (3.9)$$

provided that $\hat{\rho} \leq |a - a^{-1}|$ (a^{-1} is the radius of curvature at $l=0, \pi$).

Three distinct situations, corresponding to different values of $\hat{\rho}$, are presented in figure 2 for a prolate spheroid with $a=2$. The pedal function N (thick solid line) in the highly symmetric case $\hat{\rho}=0$, when G coincides with O, is shown in figure 2a; figure 2b shows the height function $h(\theta)$ for this case. In this case, there are four static equilibria located at the points where the pedal function is tangent to the contour S ; these points also correspond to the extremal points of the height function. When G is displaced (figure 2c,d), the intermediate equilibria move towards one of the vertical equilibria and finally disappear at one end (figure 2e,f). It will become clear in the following sections that the structure of dynamic equilibria is, in general, intimately related to the existence and location of such intermediate static equilibria.

Consider now the following family of convex axisymmetric shapes with cross-section S given by

$$S = (r_M \sin l, r_M \cos l) \quad \text{with } r_M(l) = 1 + \epsilon_M \cos Ml, \quad M = 1, 2, \dots, \quad (3.10)$$

² Similar relationship can be established between the static equilibria of arbitrary convex body, the pedal surface with respect to arbitrary location of the pedal point G (centre-of-mass), and a two-parameter function $Q(l, k)$.

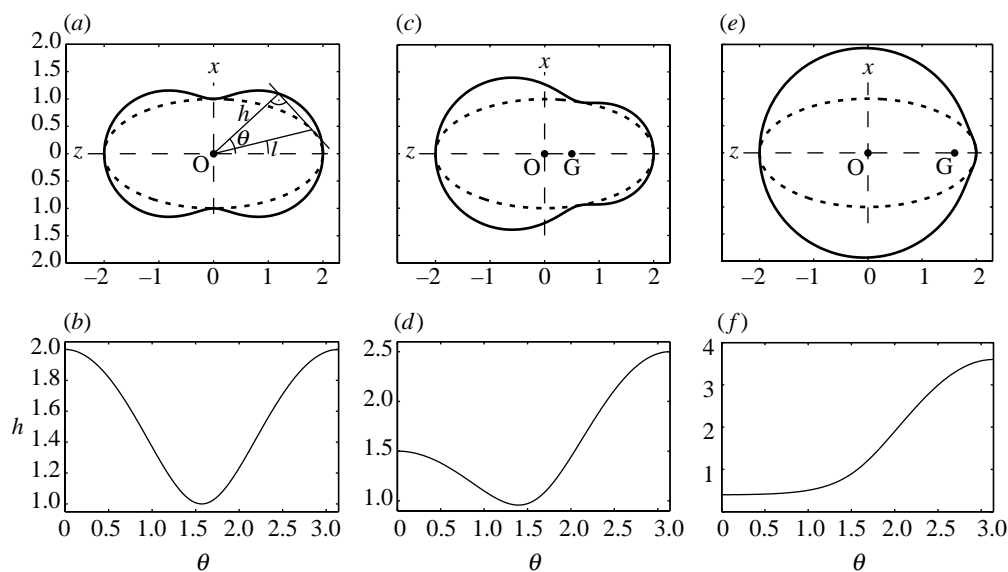


Figure 2. Pedal curves N (thick solid) given by (3.8) and height functions h (3.5) for a prolate spheroid (thick dashed) with $a=2$ and different locations of the pedal point $G = (0, \hat{\rho})$ (i.e. centre-of-mass in $Oxyz$; see figure 1) (a,b) $\hat{\rho} = 0$, (c,d) $\hat{\rho} = -0.5$, (e, f) $\hat{\rho} = -1.6$. Static equilibria are located at points where the pedal curve is tangent to the contour S (3.7); these equilibria correspond to the points where $dh/d\theta = 0$ (b,d,f).

where $l \in [0, 2\pi]$ and

$$\epsilon_M < (M^2 + 1)^{-1}. \quad (3.11)$$

In this case, the pedal curve of S with respect to $G = (0, \hat{\rho})$ can be obtained by substituting (3.10) into (3.3); a few examples are shown in figure 3. The static equilibria are determined by the solution of (3.4) which, in combination with (3.10), takes the form

$$(r_M(l)\sin l + M\epsilon_M \sin Ml \cos l)\hat{\rho} - M\epsilon_M r_M(l)\sin Ml = 0. \quad (3.12)$$

There are at most $2M$ static equilibria in this case which, for $\hat{\rho} = 0$, are located at

$$l_m^{(0)} = \frac{\pi m}{M}, \quad m = 0, 1, \dots, 2M-1. \quad (3.13)$$

For $|\hat{\rho}| \ll 1$, these roots are, generally, perturbed to

$$l_m = l_m^{(0)} + (-1)^m \frac{\hat{\rho} \sin(m\pi/M)}{M^2 \epsilon_M}. \quad (3.14)$$

Finally, for arbitrary $\hat{\rho}$, (3.12) has to be solved numerically. The result, along with the corresponding pedal curves and height functions, is shown in figure 3 for $M=3$. In both cases, pairs of static equilibria merge and disappear as $\hat{\rho}$ is increased, leaving eventually only the two vertical equilibria with P located on the axis of symmetry.

(b) Classification of steady states for arbitrary convex geometry

We can now determine all steady states satisfying (3.1). As was shown in part I, when slipping friction is present between the spinning body and the table,

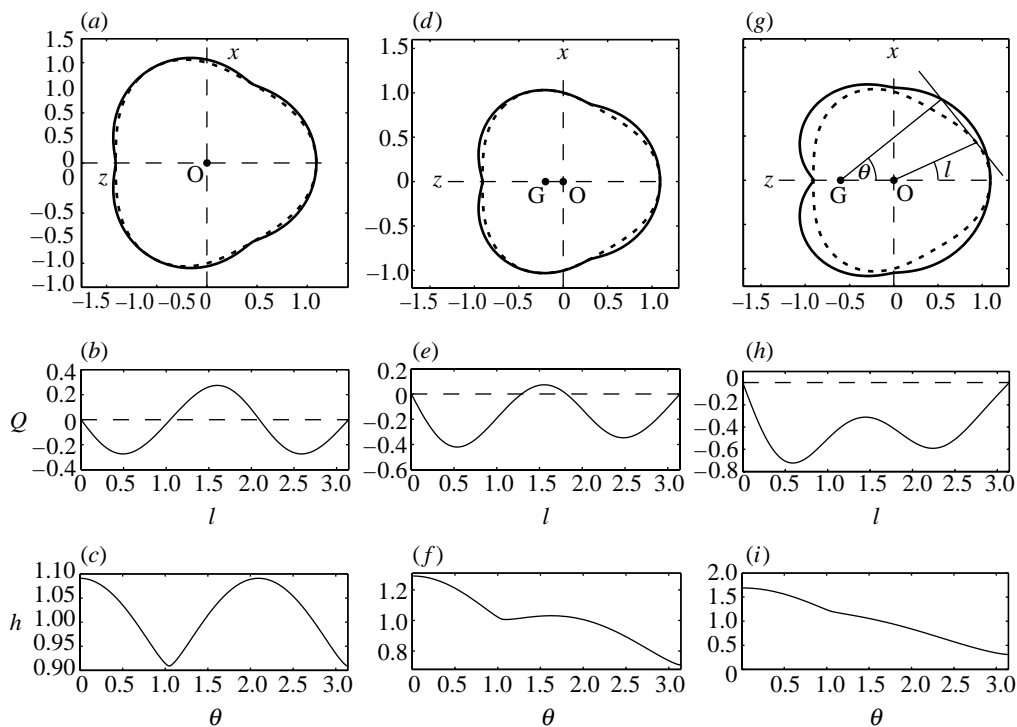


Figure 3. Pedal curves N (thick solid) and height functions h for an axisymmetric body with cross-section S (thick dashed) given by (3.10) with $M=3$, $\epsilon_M = 1/(M^2 + 2)$ and different locations of the pedal point $G = (0, \hat{\rho})$ (i.e. centre-of-mass in $Oxyz$): (a–c) $\hat{\rho} = 0$, (d–f) $\hat{\rho} = 0.18$, (g–i) $\hat{\rho} = 0.6$; see figure 2. Static equilibria correspond to the points where $dh/d\theta = 0$ or, equivalently, are given by $Q(l) = 0$, where the pedal curve is tangent to the contour S (see (3.4)); $\theta(l)$ is given by (3.6).

the energy of the system (2.7a–f) is dissipated according to

$$\frac{dE}{dt} = -\mu R \mathbf{U}_P \cdot \mathbf{f}(\mathbf{U}_P). \quad (3.15)$$

In a steady state with $\mu > 0$, it therefore follows that $\mathbf{U}_P = 0$ and $\mathbf{F} = 0$; hence from (2.4a–c), (3.1) and (2.7a–f) it follows that

$$U = W = \Omega V = A = 0. \quad (3.16)$$

Furthermore, from (2.4b) and (2.7d), we find that $R = 1$ and

$$V + h \sin \theta (n - \Omega \cos \theta) + h_\theta (n \cos \theta + \Omega \sin^2 \theta) = 0, \quad (3.17)$$

and

$$(A\Omega \cos \theta - Cn)\Omega \sin \theta = h_\theta. \quad (3.18)$$

Equations (3.16), (3.17) and (3.18) have a number of solutions which may be classified as follows.

Static equilibria

In these states, as discussed above, the body is at rest on the table ($U = V = \Omega = A = n = 0$), with axis of symmetry inclined to the vertical at discrete equilibrium angles θ_e such that $h_{\theta_e} (= dh/d\theta|_{\theta=\theta_e}) = 0$.

Dynamic equilibria

(i) *Vertical spin states.* These states represent spin about the axis of symmetry in the vertical orientation and satisfy:

$$U = V = A = 0, \quad \theta = \begin{cases} 0, \\ \pi, \end{cases} \quad n \text{ arbitrary, } \Omega \text{ undefined.} \quad (3.19)$$

They are, in some sense, degenerate since Ω is not defined at $\theta=0, \pi$. This degeneracy is to be expected, since the choice of the Euler angle coordinates is not a diffeomorphism on $SO(3)$. Note also that the two vertical static equilibria are connected to this class. These states are always present in the phase space, since we assumed $h_\theta=0$ at $\theta=0, \pi$.

(ii) *Intermediate states.* These correspond to solutions for which $U=V=A=0$ and $0<\theta<\pi$. For such states

$$\Omega^2 = \frac{h_\theta[h \sin \theta + h_\theta \cos \theta]}{\sin \theta[\cos \theta \sin \theta(A-C)h + (A \cos^2 \theta + C \sin^2 \theta)h_\theta]}, \quad (3.20)$$

and

$$n = \frac{\Omega \sin \theta[h \cos \theta - h_\theta \sin \theta]}{h \sin \theta + h_\theta \cos \theta}. \quad (3.21)$$

Note first that intermediate states exist only in intervals $\tilde{\theta}$ within which the right-hand side of (3.20) is positive. In the particular (non-generic) situation when $A=C$, we find that $\tilde{\theta}=(0, \pi)$ and there is a single branch of such states connecting two vertical spin states at $\theta=0$ and π . If $A \neq C$, the number and location of intermediate-state branches depends on the distribution of roots of the numerator and the denominator in (3.20), and on the signs of the first derivatives at these roots. Consequently, the resulting fixed-point structure can be arbitrarily complex in general. There are, however, a few important characteristics of the intermediate-state branches which provide a key to understanding the overall structure.

Note first that the numerator of (3.20) vanishes at the points θ_e , where $h_{\theta_e}=0$, which also determines the location of the static equilibria given by ($U=V=\Omega=A=n=0, \theta=\theta_e$). Thus, for $A \neq C$, every static equilibrium corresponding to an extremum of the height function ($h_{\theta_e}=0, h_{\theta\theta_e} \neq 0$), except $\theta_e=0, \pi/2, \pi$, is connected in the phase space to a branch of intermediate states. As discussed in §3a, there may be arbitrarily many static equilibria for a general axisymmetric body and the corresponding structure of the intermediate-state branches can be arbitrarily complex.

From (3.21), we see that if the equation

$$z_p = h_\theta \sin \theta - h \cos \theta = 0 \quad (3.22)$$

has solutions for $0 < \theta_{pr} < \pi/2$ or $\pi/2 < \theta_{pr} < \pi$ and $\theta_{pr} \in \tilde{\theta}$, then a branch of intermediate states crosses the plane $n=0$ at the fixed-point of ‘pure precession’ located at

$$U = V = A = n = 0, \quad \theta = \theta_{pr}, \quad \Omega_{pr}^2 = \frac{h(\theta_{pr})}{A \sin^2 \theta_{pr}}. \quad (3.23)$$

If, however, $\theta_{\text{pr}} = \theta_e = \pi/2$ and $\pi/2 \in \tilde{\theta}$, then a branch of intermediate states crosses the plane $n=0$ at

$$U = V = A = n = 0, \quad \theta_e = \pi/2, \quad \Omega_e^2 = \mathcal{K}^{-1}, \quad (3.24)$$

where

$$\mathcal{K} = \frac{(h_{\pi/2} + h_{\theta\theta_{\pi/2}})C - Ah_{\pi/2}}{h_{\pi/2}h_{\theta\theta_{\pi/2}}}, \quad (3.25)$$

and $h_{\pi/2} = h(\pi/2)$ and $h_{\theta\theta_{\pi/2}} = d^2h/d\theta^2|_{\theta=\pi/2}$. (If $\mathcal{K} < 0$, we see from (3.20) that $\pi/2 \notin \tilde{\theta}$.) It is then clear, from (3.23) and (3.24), that $\Omega_{\text{pr}} \neq \Omega_e$ unless $A = C$. Moreover, the static equilibrium at $\theta_e = \pi/2$ is disconnected from the intermediate states. This discontinuous behaviour is caused by the appearance of horizontal-precession states (see (iii) below) which lie entirely in the plane $n=0$ at $\theta = \pi/2$. Note that part I was entirely devoted to a degenerate situation of this kind which arises in the case of a uniform flip-symmetric spheroid.

Provided $A \neq C$ and $\theta_e \neq \pi/2$, a branch of intermediate states has asymptotes at points θ_∞ , where the denominator of (3.20) vanishes, i.e. where

$$\frac{h_\theta}{h} = \frac{(C - A)\cos\theta\sin\theta}{A\cos^2\theta + C\sin^2\theta}. \quad (3.26)$$

These points determine the location of intermediate equilibria in the ‘gyroscopic region’ ($\Omega \rightarrow \infty$).

Note finally that in the limit $\theta \rightarrow 0$ we obtain

$$\Omega_0^2 = \frac{h_{\theta\theta|_0}(h_0 + h_{\theta\theta|_0})}{A(h_0 + h_{\theta\theta|_0}) - Ch_0}, \quad n_0 = \frac{h_0\Omega_0}{h_0 + h_{\theta\theta|_0}}, \quad (3.27)$$

and for $\theta \rightarrow \pi$ we get

$$\Omega_\pi^2 = \frac{h_{\theta\theta|\pi}(h_\pi + h_{\theta\theta|\pi})}{A(h_\pi + h_{\theta\theta|\pi}) - Ch_\pi}, \quad n_\pi = -\frac{h_\pi\Omega_\pi}{h_\pi + h_{\theta\theta|\pi}}, \quad (3.28)$$

provided the right-hand side of (3.20) is positive at these points.

(iii) *Arbitrary precession states.* We can distinguish two subcategories here. First, the ‘horizontal precession states’ exist only if $dh/d\theta|_{\theta=\pi/2} = 0$.³ Then, equations (3.17) and (3.18) have an additional solution of the form

$$U = V = A = n = 0, \quad \theta = \pi/2, \quad \Omega \text{ arbitrary}, \quad (3.29)$$

representing a steady motion in which the axis of symmetry rotates in a horizontal plane with precessional angular velocity Ω . Provided that $\mathcal{K} > 0$ (see (3.25)), the line of horizontal-precession states intersects a branch of intermediate states at ($\Omega = \mathcal{K}^{-1/2}$, $\theta = \pi/2$, $n = 0$) and is connected to the static equilibrium at ($U = V = \Omega = A = n = 0$, $\theta = \pi/2$).

The second subcategory of arbitrary precession states exists in the non-generic situation, when $A = C$ and $dh/d\theta|_{\theta=\theta_e} = 0$ ($\theta_e \neq 0, \pi$). Then, equations (3.17) and (3.18) have an additional solution of the form:

$$U = V = A = 0, \quad \theta = \theta_e, \quad n = \Omega \cos\theta_e, \quad \Omega \text{ arbitrary}. \quad (3.30)$$

This branch originates at the static equilibrium ($U = V = \Omega = A = n = 0$, $\theta = \theta_e$) and intersects the branch of intermediate states at ($\Omega_e^2 = h(\theta_e)/A$, $\theta = \theta_e$, $n = \Omega_e \cos\theta_e$).

³Note that the body need not be flip-symmetric in such a case.

(iv) *Rolling states (zero-precession)*. These states exist if the height function has an additional extremum at $0 < \theta_e < \pi$ (so that $dh/d\theta|_{\theta=\theta_e} = 0$). Then, the body remains inclined at the angle θ_e to the vertical and rolls on the table without precession. In such a case, we obtain

$$U = \Omega = \Lambda = 0, \quad \theta = \theta_e, \quad V = -h_e \sin \theta_e n, \quad n \text{ arbitrary}, \quad (3.31)$$

where $h_e = h(\theta_e)$. Note that the rolling states, if they exist, are connected to a branch of the intermediate states through a static equilibrium located at $\mathcal{E}_e = (U = V = \Omega = \Lambda = n = 0, \theta_e)$.

Geometrically, the classes (i)–(iv) represent branches of non-isolated fixed-points, embedded in the subspace (V, Ω, θ, n) of the six-dimensional phase space \mathcal{E} , and the static equilibria serve as points of connection between these branches. Note that the topology of the resulting global structure is determined by the height function h and the principal moments of inertia A, C , and may be complex in the general case. We study such structures and their bifurcations for two important, though relatively simple, examples in §4.

4. Geometry of the fixed-point structures

These two examples are: the spheroid with displaced centre-of-mass and the tippe-top. In both cases, we follow the analysis of §3 using an appropriate height function h . It will be shown in a subsequent paper (part IV in this series) that the geometrical approach presented here is particularly useful in studying global aspects of the spinning body dynamics.

(a) Spheroid with displaced centre-of-mass

The case of a flip-symmetric spheroid of axisymmetric density distribution was considered in part I. When the centre-of-mass is displaced with respect to the centre-of-volume by a distance $0 \leq \hat{\rho} \leq a$, the height function h is given by

$$h(\theta) = (a^2 \cos^2 \theta + \sin^2 \theta)^{1/2} - \hat{\rho} \cos \theta, \quad (4.1)$$

where, as before, a is the ratio of the principal axes of the spheroid.

The first and second derivatives, which will be needed later, are respectively

$$h_\theta = \frac{dh}{d\theta} = -\frac{(a^2 - 1)\sin \theta \cos \theta}{\sqrt{a^2 \cos^2 \theta + \sin^2 \theta}} + \hat{\rho} \sin \theta \quad (4.2)$$

and

$$h_{\theta\theta} = \frac{d^2 h}{d\theta^2} = \frac{(a^2 - 1)(\sin^4 \theta - a^2 \cos^4 \theta)}{(a^2 \cos^2 \theta + \sin^2 \theta)^{3/2}} + \hat{\rho} \cos \theta. \quad (4.3)$$

Note that if $a=1$, (4.1)–(4.3) describe the geometry of the tippe-top; we shall discuss this case in detail in §4b.

Using (4.1)–(4.3) and the results of §3, the steady states for the spheroid with displaced centre-of-mass can now be described as follows:

Static equilibria

There are at most three distinct static equilibria in this case: two ‘vertical’ equilibria, when $\theta_e = 0$ or π , and one ‘intermediate’ equilibrium when the axis of symmetry is inclined to the vertical at the angle θ_N given by (4.9).

(i) *Vertical spin states* are given by (3.19).

In the ‘non-risen’ state, when $\theta=0$, the centre-of-mass remains at the height $h_0 = a - \hat{\rho}$. In the ‘risen’ state, when $\theta=\pi$, $h_\pi = a + \hat{\rho}$.

(ii) *Intermediate states*. Provided $a^2 C = A \neq 0$ and $C\hat{\rho} \neq 0$,⁴ substitution of (4.1)–(4.3) into (3.21), (3.20) yields

$$\Omega^2 = \frac{(a^2 - 1)\cos\theta - \hat{\rho}\mathcal{H}}{\mathcal{H}((a^2 C - A)\cos\theta - C\hat{\rho}\mathcal{H})} = \frac{\mathcal{N}}{\mathcal{H}\mathcal{D}}, \quad (4.4)$$

and

$$n = \Omega(a^2 \cos\theta - \hat{\rho}\mathcal{H}), \quad (4.5)$$

where \mathcal{H} , \mathcal{N} and \mathcal{D} are defined as

$$\mathcal{H} = (a^2 \cos^2\theta + \sin^2\theta)^{1/2}, \quad (4.6)$$

$$\mathcal{N} = (a^2 - 1)\cos\theta - \hat{\rho}\mathcal{H}, \quad \mathcal{D} = (a^2 C - A)\cos\theta - C\hat{\rho}\mathcal{H}. \quad (4.7)$$

These states, generally, lie on separate branches and the particular configuration is controlled by four parameters $(A, C, a, \hat{\rho})$. Note first that if $A=C$, we obtain $\mathcal{N}=\mathcal{D}$ and there is a single branch, spanned between $\theta=0$ and π , which can be written as

$$\Omega = \frac{1}{C\mathcal{H}}, \quad n = \frac{a^2 \cos\theta - \hat{\rho}\mathcal{H}}{\sqrt{C\mathcal{H}}}. \quad (4.8)$$

For $A \neq C$, the branch configuration is determined by location of roots $\theta_{\mathcal{N}}$, $\theta_{\mathcal{D}}$ and values of the first derivatives at these roots $\mathcal{N}_{\theta_{\mathcal{N}}} = (d\mathcal{N}/d\theta)|_{\theta=\theta_{\mathcal{N}}}$, $\mathcal{D}_{\theta_{\mathcal{D}}} = (d\mathcal{D}/d\theta)|_{\theta=\theta_{\mathcal{D}}}$, which we derive below.

The numerator of (4.4) has a single zero at

$$\theta_{\mathcal{N}} = \begin{cases} \tan^{-1}[(a^4 - (2 + \rho^2)a^2 + 1)^{1/2}\hat{\rho}^{-1}], & \text{if } a > 1, \\ \pi - \tan^{-1}[(a^4 - (2 + \rho^2)a^2 + 1)^{1/2}\hat{\rho}^{-1}], & \text{if } a < 1, \end{cases} \quad (4.9)$$

provided that

$$\hat{\rho} \leq \rho_c \begin{cases} (a^2 - 1)a^{-1}, & \text{if } a > 1 \text{ (prolate spheroid),} \\ (1 - a^2)a^{-1}, & \text{if } \sqrt{2}/2 < a < 1 \text{ (oblate spheroid),} \\ a, & \text{if } a < \sqrt{2}/2 \text{ (oblate spheroid).} \end{cases} \quad (4.10)$$

Note that $\theta_{\mathcal{N}}$ determines the locations of an ‘intermediate’ static equilibrium; for $\theta_{\mathcal{N}} \neq \pi/2$, a branch of intermediate fixed-points originates from such a point. If $\hat{\rho} \geq \rho_c$, or if $a=1$, $\theta_{\mathcal{N}}$ does not exist, \mathcal{N} remains negative and there are only two ‘vertical’ static equilibria present in the system.

The first derivative of \mathcal{N} can be written

$$\mathcal{N}_{\theta} \equiv \frac{d\mathcal{N}}{d\theta} = (1 - a^2)\sin\theta \left(1 - \frac{\hat{\rho}\cos\theta}{\mathcal{H}}\right) \begin{cases} > 0, & \text{if } a < 1, \\ < 0, & \text{if } a > 1, \end{cases} \quad (4.11)$$

⁴In such a degenerate case, we obtain from (3.17) and (3.18) that $(\theta=\pi/2, n=0, \Omega \text{ arbitrary})$, which belongs to the class of horizontal states.

and its sign is independent of θ and $\hat{\rho}$. The asymptote of the intermediate-states branch is located at

$$\theta_{\mathcal{D}} = \begin{cases} \tan^{-1} \sqrt{\chi^2 - a^2}, & \text{if } \chi > 0, \\ \pi - \tan^{-1} \sqrt{\chi^2 - a^2}, & \text{if } \chi < 0, \end{cases} \quad (4.12)$$

provided that

$$C\hat{\rho} \neq 0, \quad |\chi| = \left| \frac{a^2 C - A}{C\hat{\rho}} \right| \geq a. \quad (4.13)$$

In the special case when

$$C\hat{\rho} = 0, \quad a^2 C - A \neq 0, \quad (4.14)$$

the denominator vanishes at $\theta_{\mathcal{D}} = \pi/2$. Otherwise, $\theta_{\mathcal{D}}$ does not exist \mathcal{D} remains negative, and there are no intermediate states in the gyroscopic region ($\Omega \gg 1$) of the phase space. The first derivative of \mathcal{D} can be expressed as

$$\mathcal{D}_{\theta} \equiv \frac{d\mathcal{D}}{d\theta} = \frac{[(A - a^2 C)\mathcal{H} + (a^2 - 1)C\hat{\rho} \cos \theta] \sin \theta}{\mathcal{H}}. \quad (4.15)$$

Finally, evaluation of (4.5) at $\theta_{\mathcal{D}}$ (4.12) leads to

$$\mathcal{D}_{\theta_{\mathcal{D}}} = \left(\frac{d\mathcal{D}}{d\theta} \right)_{\theta=\theta_{\mathcal{D}}} \begin{cases} < 0, & \text{if } C\hat{\rho} \neq 0, \chi > a, \\ > 0, & \text{if } C\hat{\rho} \neq 0, \chi < -a, \\ \text{sgn}(a^2 C - A), & \text{if } C\hat{\rho} = 0, a^2 C - A \neq 0. \end{cases} \quad (4.16)$$

Combining the information about $\theta_{\mathcal{N}}$, $\theta_{\mathcal{D}}$, $\mathcal{N}_{\theta_{\mathcal{N}}}$ and $\mathcal{D}_{\theta_{\mathcal{D}}}$ leads to nine topologically distinct configurations of the fixed-point structures which we describe below (see also figures 4 and 5). Similar procedures could be used to classify the fixed-point structures for other axisymmetric bodies.

- (1) Conditions (4.10) and (4.13) are not satisfied (the numerator \mathcal{N} and the denominator \mathcal{D} of (4.4) do not vanish at any point within $0 < \theta < \pi$).

$\theta_{\mathcal{N}}$ does not exist, $\theta_{\mathcal{D}}$ does not exist, $\mathcal{N} \cdot \mathcal{D} > 0$. There is a single branch of non-isolated fixed-points that connects the states of vertical spin with $(\Omega_0, \theta=0, n_0)$ and $(\Omega_{\pi}, \theta=\pi, n_{\pi})$, where

$$\Omega_0^2 = \frac{a(a - \hat{\rho}) - 1}{a(aC(a - \hat{\rho}) - A)}, \quad n_0 = \Omega_0 a(a - \hat{\rho}), \quad (4.17)$$

$$\Omega_{\pi}^2 = \frac{a(a + \hat{\rho}) - 1}{a(aC(a + \hat{\rho}) - A)}, \quad n_{\pi} = -\Omega_{\pi} a(a + \hat{\rho}). \quad (4.18)$$

Note that n_0 and n_{π} always have opposite signs and that the rolling states do not exist in this configuration.

- (2) $\theta_{\mathcal{D}}$ does not exist, $\mathcal{D}(\theta_{\mathcal{N}}) \cdot \mathcal{N}_{\theta_{\mathcal{N}}} < 0$ (condition (4.10) satisfied, condition (4.13) not satisfied). There is a single branch connecting the non-risen vertical spin state with $(\Omega_0, \theta=0, n_0)$ with the static equilibrium $(\Omega=0, \theta_{\mathcal{N}}, n=0)$. This configuration can be realized only for oblate spheroids ($a < 1$).
- (3) $\theta_{\mathcal{D}}$ does not exist, $\mathcal{D}(\theta_{\mathcal{N}}) \cdot \mathcal{N}_{\theta_{\mathcal{N}}} > 0$. There is a single branch connecting the static equilibrium $(\Omega=0, \theta_{\mathcal{N}}, n=0)$ with the risen vertical spin state $(\Omega_{\pi}, \theta=\pi, n_{\pi})$. This branch exists only for prolate spheroids ($a > 1$).

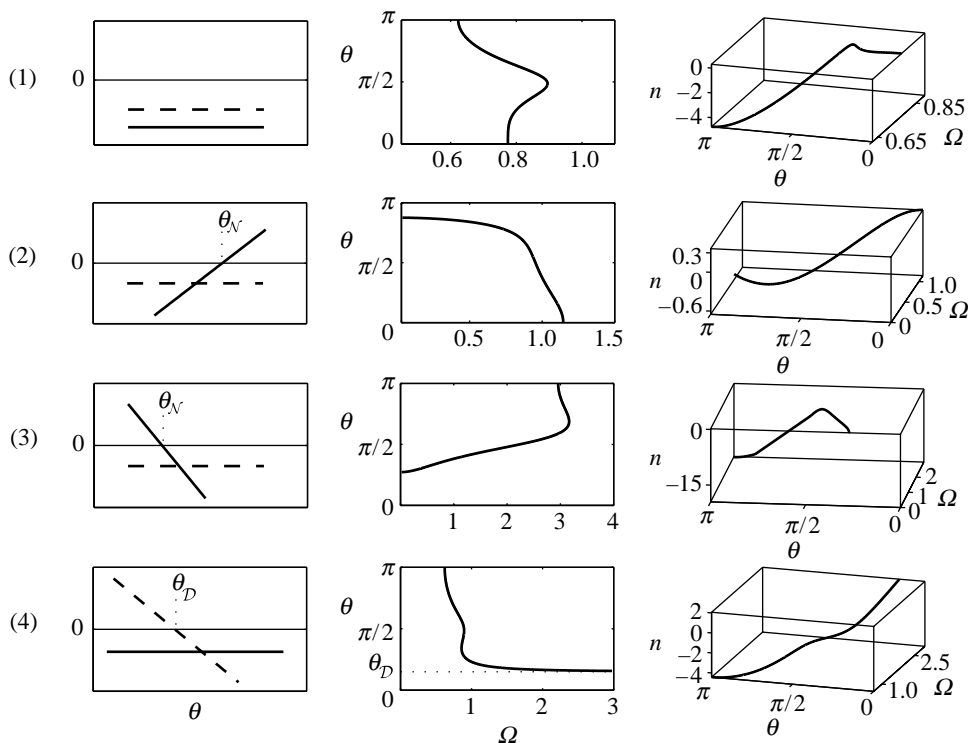


Figure 4. Structures of non-isolated intermediate fixed-points for a spheroid with displaced centre-of-mass. Distinct classes are shown that depend on the parameters $(A, C, a, \hat{\rho})$. The first column represents schematically the numerator \mathcal{N} (solid) and the denominator \mathcal{D} (dashed) of (4.4) near the zero-crossing. The second column shows the projection of the fixed-point line onto (Ω, θ) and the third column shows the three-dimensional geometry in the subspace (Ω, θ, n) of the six-dimensional phase space Ξ in which these fixed-points are always embedded. Class: (1) $A=1$, $C=1.25$, $a=2$, $\hat{\rho}=1.8$, $\rho_c=1.5$, $\chi=1.78$; (2) $A=1$, $C=1.1$, $a=0.8$, $\hat{\rho}=0.4$, $\rho_c=0.45$, $\chi=-0.67$; (3) $A=1$, $C=0.2$, $a=2$, $\hat{\rho}=1.3$, $\rho_c=1.5$, $\chi=2.06$; (4) $A=1$, $C=1.25$, $a=2$, $\hat{\rho}=1.55$, $\rho_c=1.5$, $\chi=2.06$. Note that these are just particular examples. Continued on [figure 5](#).

- (4) $\theta_{\mathcal{N}}$ does not exist, $\mathcal{N}(\theta_{\mathcal{D}}) \cdot \mathcal{D}_{\theta_{\mathcal{D}}} > 0$ (condition (4.10) not satisfied, condition (4.13) satisfied). There is a single branch originating at the vertical state $(\Omega_{\pi}, \theta = \pi, n_{\pi})$ which has an asymptote at $\theta = \theta_{\mathcal{D}}$. There are no intermediate-angle static equilibria or rolling states in this configuration.
- (5) $\theta_{\mathcal{N}}$ does not exist, $\mathcal{N}(\theta_{\mathcal{D}}) \cdot \mathcal{D}_{\theta_{\mathcal{D}}} < 0$ ((4.10) not satisfied, (4.13) satisfied). There is a single branch originating at the non-risen vertical states with $(\Omega_0, \theta = \pi, n_0)$ that has asymptote at $\theta = \theta_{\mathcal{D}}$. There are no intermediate angle static equilibria or rolling states in this configuration.
- (6) $\theta_{\mathcal{N}} \neq \theta_{\mathcal{D}}$ and $\mathcal{N}_{\theta_{\mathcal{N}}} \cdot \mathcal{D}_{\theta_{\mathcal{D}}} < 0$. There is a single branch that originates at the static equilibrium $(\theta = \theta_{\mathcal{N}}, \Omega = 0, n = 0)$ and has an asymptote at $\theta = \theta_{\mathcal{D}}$.

Note that if $\theta_{\mathcal{N}} = \theta_{\mathcal{D}}$ and $\mathcal{N}_{\theta_{\mathcal{N}}} \cdot \mathcal{D}_{\theta_{\mathcal{D}}} < 0$ (i.e. $\mathcal{K} < 0$ in (3.25)), there are no intermediate fixed-points in the phase space. (There exists, however, a line of horizontal-precession states.)

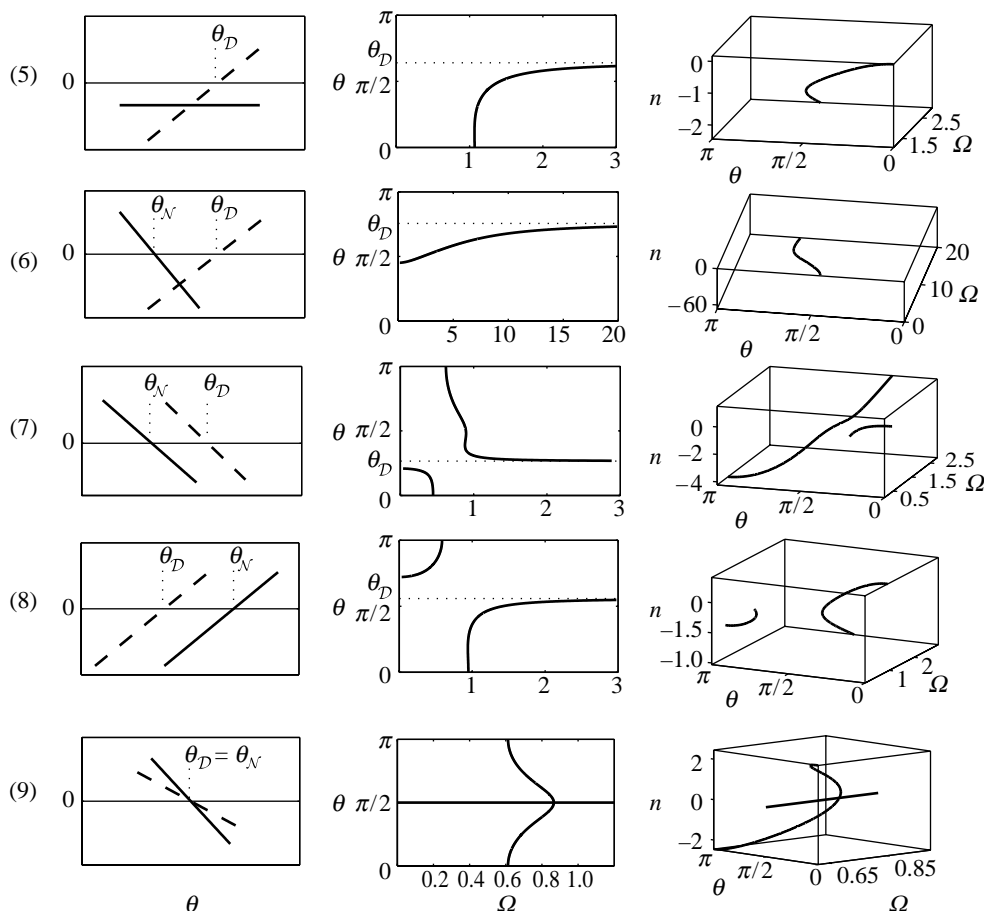


Figure 5. (continuation of figure 4) Structures of non-isolated intermediate fixed-points for a spheroid with displaced centre-of-mass. (5) $A=1$, $C=0.5$, $a=0.8$, $\hat{\rho}=0.6$, $\rho_c=0.45$, $\chi=2.27$; (6) $A=1$, $C=0.2$, $a=2$, $\hat{\rho}=0.45$, $\rho_c=1.5$, $\chi=2.22$; (7) $A=1$, $C=1.25$, $a=2$, $\hat{\rho}=1.4$, $\rho_c=1.5$, $\chi=2.28$; (8) $A=1$, $C=0.5$, $a=0.8$, $\hat{\rho}=0.25$, $\rho_c=0.45$, $\chi=5.44$ and (9) $A=1$, $C=1.25$, $a=2$, $\hat{\rho}=0$, χ undefined.

- (7) $\theta_N < \theta_D$ and $\mathcal{N}_{\theta_N} \cdot \mathcal{D}_{\theta_D} > 0$. There are two distinct branches: one branch connects the non-risen vertical spin state $(\Omega_0, \theta=0, n_0)$ with the static equilibrium $(\Omega=0, \theta=\theta_N, n=0)$ and the other branch originates at the risen vertical state $(\Omega_\pi, \theta=\pi, n_\pi)$ and has an asymptote at $\theta=\theta_D$.
- (8) $\theta_N > \theta_D$ and $\mathcal{N}_{\theta_N} \cdot \mathcal{D}_{\theta_D} > 0$. Two branches exist; one branch originates at the non-risen vertical spin state $(\Omega_0, \theta=0, n_0)$ and has asymptote at $\theta=\theta_D$ and the other branch connects the rolling state with $(\Omega=0, \theta=\theta_N, n=0)$ with the risen vertical spin state at $(\Omega_\pi, \theta=\pi, n_\pi)$.
- (9) If $\theta_N = \theta_D = \theta_*$, and $\lim_{\theta \rightarrow \theta_*} 0 < \mathcal{N}_\theta / \mathcal{D}_\theta < \infty$. In this special case, the two branches ‘reconnect’ to form a structure which always exists in combination with the line of horizontal-precession states located at $(\Omega, \theta=\pi/2, n=0)$. This configuration, characteristic of flip-symmetric bodies, was discussed in part I.

Figure 6 shows location of the topology classes (1)–(9) in the parameter subspace $(a, \hat{\rho})$ for three distinct cases $A < C$, $A = C$ and $A > C$. The thick curves mark the solutions $\chi = a$ and $-a$ (see (4.13)); the region between these curves corresponds to $|\chi| \leq a$. The thin curves correspond to the solutions $\hat{\rho} = \rho_c$ (see (4.10)) and the region enclosed by these curves corresponds to $\hat{\rho} \geq \rho_c$.⁵ Consequently, the topology classes (1)–(9) can be characterized in the following way.

| class | prolate case ($a > 1$, $C \neq 0$) | oblate case ($a < 1$, $C \neq 0$) | degenerate case ($C = 0$, $A \neq 0$) |
|-------|--|---|---|
| (1) | $ \chi < a$, $\hat{\rho} > \rho_c$ | $a > \sqrt{2}/2$, $ \chi < a$, $\hat{\rho} > \rho_c$ | |
| (2) | | $ \chi < a$, $0 < \hat{\rho} < \rho_c$ | |
| (3) | $ \chi < a$, $0 < \hat{\rho} < \rho_c$ | | |
| (4) | $\chi > a$, $\hat{\rho} > \rho_c$ | $a > \sqrt{2}/2$, $\chi > a$, $\hat{\rho} > \rho_c$ | |
| (5) | $\chi < -a$, $\hat{\rho} > \rho_c$ | $a > \sqrt{2}/2$, $\chi < -a$, $\hat{\rho} > \rho_c$ | $a > \sqrt{2}/2$, $\hat{\rho} > \rho_c$ |
| (6) | $\chi < -a$, $0 < \hat{\rho} < \rho_c$ | $a > \sqrt{2}/2$, $\chi > a$, $0 < \hat{\rho} < \rho_c$ | $a > 1$, $0 < \hat{\rho} < \rho_c$ |
| (7) | $A < C$, $ \chi > a$, $0 < \hat{\rho} < \rho_c$ | $A < C$, $ \chi > a$, $0 < \hat{\rho} < \rho_c$ | |
| (8) | $A > C$, $ \chi > a$, $0 < \hat{\rho} < \rho_c$ | $A > C$, $ \chi > a$, $0 < \hat{\rho} < \rho_c$ | $a < 1$, $0 < \hat{\rho} < \rho_c$ |
| (9) | $\hat{\rho} = 0$, $a^2 C - A > 0$ | $\hat{\rho} = 0$, $a^2 C - A < 0$ | $a < 1$, $\hat{\rho} = 0$ |

Figure 6 provides a convenient way of determining bifurcations of the topology classes when the system parameters are varied. Note, in particular, that there are two degenerate configurations of fixed-point structures, corresponding to the surfaces $\hat{\rho} = 0$ and $A = C$ in the parameter space, which are destroyed for any perturbation orthogonal to these surfaces.

It will be shown in the subsequent part IV in this series that, if we additionally restrict the problem to either oblate ($a < 1$) or prolate ($a > 1$) geometry, each of the topology classes (1)–(9) has distinct stability properties which lead to different dynamical behaviour within each class.

(iii) *Precession states.* In the flip-symmetric case, when $\hat{\rho} = 0$, a line of non-isolated horizontal-precession states (Ω , $\theta = \pi/2$, $n = 0$) exists in the phase space. All but one of these states disappear when the symmetry is broken ($\hat{\rho} \neq 0$). The remaining fixed-point of ‘pure precession’ (3.23) is then located on a branch of intermediate states and, for this particular geometry, is given by

$$\theta_{\text{pr}} = \tan^{-1} \left[\frac{(a^2 - \hat{\rho}^2)^{1/2} a}{\hat{\rho}} \right], \quad \Omega_{\text{pr}}^2 = \frac{1}{A\mathcal{H}(\theta_{\text{pr}})}, \quad n = 0. \quad (4.19)$$

As can be easily seen in figure 6, the horizontal-precession states can disappear in two different bifurcations depending on the actual geometry which is characterized by the parameter \mathcal{K} (see (3.25)). If the flip-symmetry is destroyed while $\mathcal{K} > 0$, the fixed-point structure (9) bifurcates into the two disjoint branches (7) or (8). This bifurcation is accompanied by discontinuity in the

⁵ The point $(a = 1, \hat{\rho} = 0, A = C)$ corresponds to a highly degenerated case of a uniform sphere and is not considered here.

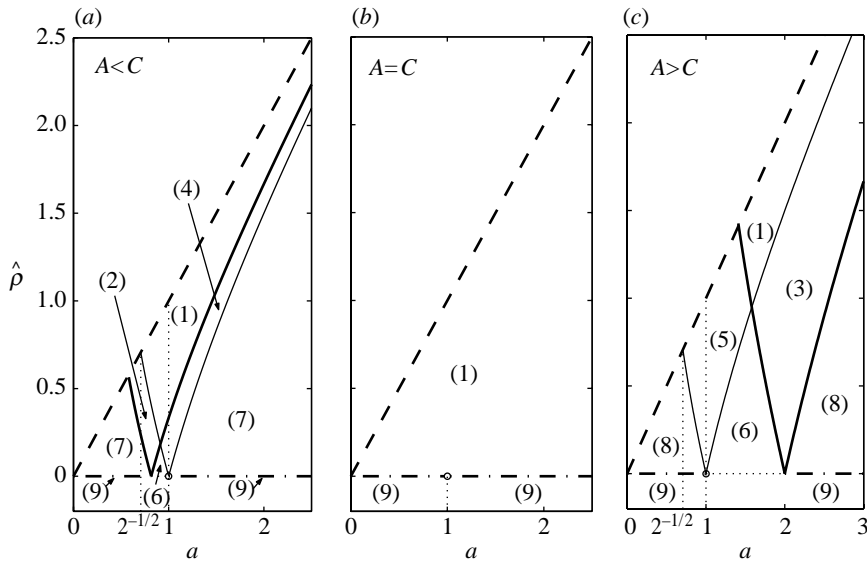


Figure 6. Location of the topology classes (1)–(8) of the intermediate fixed-points in the two-dimensional parameter subspace $(a, \hat{\rho})$; $0 \leq \hat{\rho} \leq a$. Three distinct cases are presented: (a) $A < C$ ($A=1, C=1.5$ used here), (b) $A=C$, (c) $A > C$ ($A=4, C=1$ used here). The thin solid curves, which both reach $\hat{\rho} = 0$ at $a=1$, represent the solution $\hat{\rho} = \rho_c$ (see (4.10)) and the thick solid curves, which intersect at $(\hat{\rho} = 0, a = (A/C)^{1/2})$, represent the solutions $\chi = a$ (right branch) and $\chi = -a$ (left branch) (see (4.13)). The dash-dotted lines mark the flip-symmetric states (8). Note that, if a is restricted to either $a > 1$ or $a < 1$, there is a unique parameterization of the topology classes in terms of χ and ρ_c .

location of the point where the intermediate states, given by (4.4) and (4.5), cross the plane $n=0$. For $\hat{\rho} = 0$, the intersection point is located on the line of horizontal-precession states at

$$\theta = \pi/2, \quad \Omega_{\pi/2}^2 = \mathcal{K}^{-1} = \frac{a^2 - 1}{a^2 C - A}, \quad n = 0, \tag{4.20}$$

as can be deduced from (3.24). For $\hat{\rho} \neq 0$, one of the intermediate fixed-point branches (7) or (8) crosses the plane $n=0$ at the point of pure precession (4.19). However, in the limit $\hat{\rho} \rightarrow 0$, we find that this point is located at

$$\theta_{pr} = \pi/2, \quad \Omega_{pr}^2 = A^{-1}, \quad n = 0, \tag{4.21}$$

which, unless $A=C$, is different from (4.20).

If $\mathcal{K} < 0$, there are no intermediate states in the flip-symmetric case and, when $\hat{\rho}$ increases from zero, the line of horizontal-precession states deforms into the single branch (6), crossing the plane $n=0$ at the fixed-point of pure precession (4.19).

(iv) *Rolling states.* This class of steady states exists if the condition (4.10) is satisfied, i.e. if there is a static equilibrium $0 < \theta_e < \pi$. Then, we find from (3.31) that in the rolling states

$$U = \Omega = A = 0, \quad \theta_e = \theta_N, \quad V = -(\mathcal{H}(\theta_N) - \hat{\rho} \cos \theta_N) \sin \theta_N n, \quad n, \tag{4.22}$$

where θ_N is given by (4.9) and \mathcal{H} is defined in (4.6). Note that for $\theta_N \neq \pi/2$, these

states are connected to a branch of the intermediate states through the static equilibrium located at $(U = V = \Omega = A = n = 0, \theta_N)$. Consequently, the rolling states are always part of the fixed-point structures which belong to classes (2), (3), (6), (7), (8) or (9).

(b) *Tippe-top*

The dynamics of a tippe-top has been widely studied in the past (see, for example, Hugenholtz 1952; O'Brien & Synge 1954; Cohen 1977; Or 1994; Bou-Rabee *et al.* 2004; and references of part I). However, even in this well-known case, the connection between topological structure of the fixed-point branches and distinct dynamical properties of the spinning top was not recognized. Discussion of these issues will be continued in part IV of this series.

We model the tippe-top as a sphere with displaced centre-of-mass (i.e. $a=1$, $\hat{\rho} \neq 0$, $A \neq 0$, $\mathcal{H} \equiv 1$) and find from (4.1) and (4.2) that

$$h = 1 - \hat{\rho} \cos \theta, \quad h_\theta = \hat{\rho} \sin \theta. \quad (4.23)$$

The vertical spin states are again given by (3.19). From (4.23), we see that the horizontal-precession states and the rolling states do not exist in any configuration. Using (4.4), (4.5) and (4.23), the intermediate fixed-points can be written in this case as

$$U = V = A = 0, \quad \theta \in \tilde{\theta}, \quad \Omega^2 = \frac{\hat{\rho}}{C\hat{\rho} - (C-A)\cos \theta}, \quad n = \Omega(\cos \theta - \hat{\rho}), \quad (4.24)$$

where

$$\tilde{\theta} = \begin{cases} [0 \quad \cos^{-1}(1/\chi)], & \text{if } C > A, \\ [\cos^{-1}(1/\chi) \quad \pi], & \text{if } C < A, \end{cases} \quad \chi = \frac{C-A}{C\hat{\rho}}. \quad (4.25)$$

Note that, for a tippe-top, the fixed-point of pure precession (3.23) always exists and is located at

$$U = V = A = 0, \quad \Omega_{\text{pr}} = A^{-1/2}, \quad \theta_{\text{pr}} = \cos^{-1}\hat{\rho}, \quad n = 0. \quad (4.26)$$

There are three distinct categories of fixed-point structures in this case (see also figure 6 at $a=1$).

If $|\chi| < 1$, a single branch of non-isolated fixed-points, representative of class (1), connects the non-risen vertical spin state $(\Omega_0, \theta=0, n_0)$ with the risen vertical spin state $(\Omega_\pi, \theta=\pi, n_\pi)$, where

$$\Omega_0^2 = \frac{\hat{\rho}}{A - C(1 - \hat{\rho})}, \quad n_0 = \Omega_0(1 - \hat{\rho}), \quad (4.27)$$

$$\Omega_\pi^2 = \frac{\hat{\rho}}{C(1 + \hat{\rho}) - A}, \quad n_\pi = -\Omega_\pi(1 + \hat{\rho}). \quad (4.28)$$

If, on the other hand, $|\chi| > 1$, then a branch of intermediate states has an asymptote at

$$\theta_{\mathcal{D}} = \begin{cases} \cos^{-1}(1/\chi), & \text{if } \chi > 1, \\ \pi - \cos^{-1}(1/\chi), & \text{if } \chi < -1. \end{cases} \quad (4.29)$$

The resulting fixed-point structure belongs for $\chi > 1$ to the class (4), and for $\chi < -1$ to the class (5).

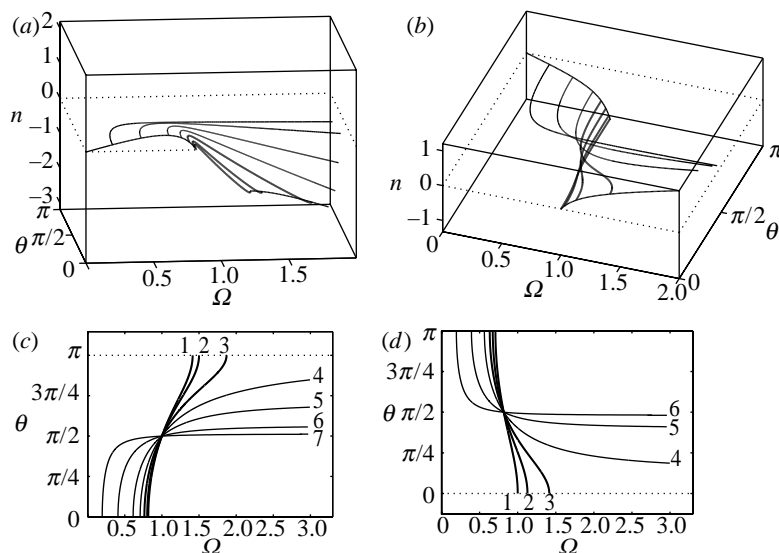


Figure 7. Intermediate steady states for a tipp-top. Geometry of the non-isolated fixed-point lines shown for (a), (c) $\chi < 0$, $A = 1.5$, $C = 1$ and $\hat{\rho} = (1) 1$, (2) 0.9, (3) 0.7, (4) 0.5, (5) 0.3, (6) 0.1, (7) 0.02; the thin solid lines represent fixed-points of the class (5) in this case; (b), (d) $\chi > 0$, $A = 1$, $C = 1.5$ and $\hat{\rho} = (1) 1$, (2) 0.7, (3) 0.5, (4) 0.3, (5) 0.1, (6) 0.02; the thin solid lines belong to the class (4) in this case. The thick solid lines represent fixed-point branches that belong to the class (1) (compare with figures 5 and 6).

A few examples of the intermediate fixed-point branches for a tipp-top are presented in figure 7. Figure 7a,c illustrate the case $\chi > 0$ and figure 7b,d show the case $\chi < 0$ for a sequence of different values of $\hat{\rho}$. Obviously, for given parameters ($\hat{\rho}$, A , C), only one such branch exists in the phase space. The location of the vertical spin states from which these branches originate can be parameterized as

$$n_0 = \Omega \frac{1 - A\Omega^2}{1 - C\Omega^2}, \quad n_\pi = -\Omega \frac{1 - A\Omega^2}{1 - C\Omega^2}, \quad (4.30)$$

where n_0 , n_π , refer to the spin values in the non-risen ($\theta = 0$) and risen ($\theta = \pi$) orientations, respectively (see figure 7).

5. Discussion and conclusions

We have sought to provide a complete geometrical description of the phase space structure of the steady states for a convex axisymmetric body of axisymmetric density distribution spinning on a horizontal table. A relationship has been established between the pedal curve of the cross-section of the body and the height function h , which allows for a straightforward determination of static equilibria for any convex body of revolution. We have shown that the number of such static equilibria can be arbitrarily large for suitable choice of body, and have identified four elementary classes of dynamic steady states in the general case. Geometrically, these states correspond to branches of non-isolated fixed-points in the six-dimensional phase space of the governing dynamical system. These

branches are usually interconnected and form a complex global structure that is determined by the height function h and the two principal moments of inertia (A , C) at the centre-of-mass G . We showed that the complexity of this structure depends on the number and location of static equilibria and on the distribution of singularities in the intermediate states.

For the prototype problem of a spheroid with displaced centre-of-mass, we have identified nine topologically distinct classes of fixed-point structures and have described their bifurcations in the parameter space $(a, \hat{\rho}, A, C)$. For the special case of the tippe-top, three such classes were identified. The simplest non-trivial case of convex flip-symmetric geometry—a spheroid with $\hat{\rho} = 0$ as considered in part I—appears within this more general framework to be a degenerate configuration that is destroyed for any $\hat{\rho} \neq 0$. In fact, any configuration containing the horizontal-precession states, including all flip-symmetric geometries, is degenerate (i.e. structurally unstable) in this sense.

This paper has prepared the way for a stability analysis of the steady states in the general case, and this will be presented in the subsequent paper (part IV in this series). In particular, it will be shown that each of the topology classes identified for the spheroid has distinct stability properties, implying different types of dynamical behaviour corresponding to the different fixed-point structures.

M.B. is supported by a scholarship from the Gates Cambridge Trust. H.K.M. acknowledges the support of a Leverhulme Emeritus Professorship. Y.S. acknowledges the support of the Keio Gijyuku Academic Development Fund.

References

- Bou-Rabee, N. M., Marsden, J. E. & Romero, L. A. 2004 Tippe top inversion as a dissipation-induced instability. *SIAM J. Appl. Dyn. Syst.* **3**, 352–377.
- Cohen, R. J. 1977 The tippe top revisited *Am. J. Phys.* **45**, 12–17.
- Hugenholtz, N. M. 1952 On tops rising by friction. *Physica* **18**, 515–527. (doi:10.1016/S0031-8914(52)80052-7)
- Moffatt, H. K. & Shimomura, Y. 2002 Spinning eggs—a paradox resolved. *Nature* **417**, 385–386. (doi:10.1038/416385a)
- Moffatt, H. K., Shimomura, Y. & Branicki, M. 2004 Dynamics of an axisymmetric body spinning on a horizontal surface. I. Stability and the gyroscopic approximation. *Proc. R. Soc. A* **460**, 3643–3672. (doi:10.1098/rspa.2004.1329)
- O'Brien, S. & Synge, J. L. 1954 The instability of the tippe top explained by sliding friction. *Proc. R. Ir. Acad. Sect. A, Math. Astron. Phys. Sci.* **56**, 23–35.
- Or, A. C. 1994 The dynamics of a tippe top. *SIAM J. Appl. Math.* **54**, 597–609. (doi:10.1137/S0036139992235123)
- Salmon, G. 1873 *A treatise on the higher plane curves*, 2nd edn. Dublin: Hodges, Foster & Co.
- Shimomura, Y., Branicki, M. & Moffatt, H. K. 2005 Dynamics of an axisymmetric body spinning on a horizontal surface. II. Self-induced jumping. *Proc. R. Soc. A* **461**, 1775–1809. (doi:10.1098/rspa.2004.1429)